Global J. Environ. Sci. Manage. 5(2): 139-154, Spring 2019

Global Journal of Environmental Science and Management
(GJESM)

Homepage: https://www.gjesm.net/

ORIGINAL RESEARCH PAPER

Flood hazard mapping in an urban area using combined hydrologic-hydraulic models and geospatial technologies

B.A.M.Talisay*, G.R. Puno, R.A.L. Amper

GeoSAFER Northern Mindanao/ Cotabato Project, College of Forestry and Environmental Science, Central Mindanao University, Musuan, Maramag, Bukidnon, Philippines

ARTICLE INFO

Article History:
Received 12 August 2018
Revised 12 November 2018
Accepted 30 November 2018

Keywords:
Geographic information system (GIS)
Inundation
Light detection and ranging
Model calibration

ABSTRACT

Flooding is one of the most occurring natural hazards every year risking the lives and properties of the affected communities, especially in Philippine context. To visualize the extent and mitigate the impacts of flood hazard in Malingon River in Valencia City, Bukidnon, this paper presents the combination of Geographic Information System, high-resolution Digital Elevation Model, land cover, soil, observed hydro-meteorological data; and the combined Hydrologic Engineering Center-Hydrologic Modeling System and River Analysis System models. The hydrologic model determines the precipitation-runoff relationships of the watershed and the hydraulic model calculates the flood depth and flow pattern in the floodplain area. The overall performance of hydrologic model during calibration was "very good fit" based on the criterion of Nash-Sutcliffe Coefficient of Model Efficiency, Percentage Bias and Root Mean Square Error – Observations Standard Deviation Ratio with the values of 0.87,-8.62 and 0.46, respectively. On the other hand, the performance of hydraulic model during error computation was "intermediate fit" using F measure analysis with a value of 0.56, using confusion matrix with 80.5% accuracy and the Root Mean Square Error of 0.47 meters. Flood hazard maps in 2, 5, 10, 25, 50 and 100-year return periods were generated as well as the number of flooded buildings in each flood hazard level and in different return periods were determined. The output of the study served as an important basis for a more informed decision and science-based recommendations in formulating local and regional policies for more effective and cost-efficient strategies relative to flood hazards.

DOI: 10.22034/gjesm.2019.02.01

INTRODUCTION

The Philippine archipelago was considered as one of the most disaster-prone areas of the world (FAO, 2011; Doroteo, 2015) due to its geographical location and physical environment (ADRC, 2009). An about 20 tropical cyclones enters the Philippine Area of Responsibility (PAR) per year (y) which have the largest impact (UNOCHA, 2017; JICA, 2015). In the last two decades, losses and damages caused by flooding have drastically increased (Acosta *et al.*, 2016). Typhoons Bopha on 2012, Haiyan on 2013, Hagupit on 2014, Koppu on 2015 and Tembin on 2017 were among of the worst and deadliest storms that hit the

*Corresponding Author:
Email: *bryanallan.talisay@gmail.com*
Tel.: +639777528771
Fax: +6388 356 1912

Note: Discussion period for this manuscript open until July 1, 2019 on GJESM website at the "Show Article.

country losing thousands of lives, damaging millions of houses, and destroying multimillion agricultural areas and properties (NDRRMC, 2012; NDRRMC, 2013; NDRRMC, 2014; NDRRMC, 2015; OCHA, 2015; Acosta *et al*., 2016; NDRRMC, 2017; LWR, 2017, IFRC, 2017). With the dire need of mitigating the impact of rainfall-induced flooding, research efforts had been conducted as a response to urgent needs of assessing environmental risks in flood-prone areas. Flood hazard assessment is a vital component in identifying vulnerable areas which needs immediate response for mitigation strategies and prevents adverse impacts in the future. Through this approach, it also helps communities and disaster managers to minimize the impacts of flooding and more efficient in determining adaptation strategies (Makinano-Santillan *et al*., 2015; Vojtek and Vojteková, 2016). One of the most extensively utilized techniques in assessing and mapping of flood hazards is through combined hydrologic, hydraulic modeling and Geographic Information System (Costas *et al*., 2017; Koutroulis and Tsanis, 2010; Kherde and Sawant, 2013). In addition, the utilization of this technologies and approaches with satellite imagery made a faster-detailed monitoring and flood mapping (Ban *et al.,* 2017; Yoshimoto and Amarnath, 2017; Jung *et al*., 2014; Haq*et al.*, 2012; Saleh and Al-Hatrushi, 2009). Combination of numerical models with state-of-the-arthigh-precision topographic surveying techniques such as the use of (Light Detection and Ranging) LiDAR technology made modeling popular in flood hazard mapping (Acosta *et al.,* 2017; Turner *et al.,* 2013; Mcdougall and Temple-Watts, 2012). Flood hazard mapping involves two components: the hydrologic simulation which determines the amount, duration and occurrence of flooding event; and the hydraulic simulation which determines the behavior of flood water in the floodplains utilized in flood mapping (USACE, 2008; USACE, 2016). The use of two-dimensional (2D) approach in flood modeling which gives detailed description of the hydraulic behavior of the river's flow dynamics is vital in understanding flood flow and provide detailed hazard mapping in the floodplains (Costabile and Macchione, 2015). Moreover, this approach are used for solving unsteady flow tasks which are more demanding for input data and they are able to simulate the extent of flooded area at different time intervals (Vojtek and Vojteková, 2016; Akbari *et al.,* 2012). In this study, the combination of Geographic Information System (GIS), high-resolution Digital Elevation Model (DEM), land cover, soil, observed hydro-meteorological data; and the combined Hydrologic Engineering Center (HEC)-Hydrologic Modeling System (HMS) and River Analysis System (RAS) models were applied in flood hazard mapping of Malingon River Basin. Flood hazard map generation of 2, 5, 10, 25, 50 and 100-year return periods were conducted and the number of flooded buildings in each flood hazard level and in different return periods were determined. The study has been conducted in an urbanized area of Valencia City, Bukidnon, Philippines in 2017.

MATERIALS AND METHODS

Description of the study area

Malingon River Basin is located in an urbanized area of Valencia City, Bukidnon in the island of Mindanao, Philippines (Fig. 1). It lies between the coordinates of 7° 55' 36.95" to 7° 59' 20.67" north latitudes and 124° 56' 0.61" to 125° 7' 12.4" east longitudes with an average elevation of 673.37 meters (m) above sea level and a total drainage area of 71.67 km^2. The climate is characterized by high relative humidity with rainy season lasting five to six months in a year (Rola *et al.,* 2004). Annual flooding occurs due to inundation of Malingon River, specifically during the rainy seasons from the month of September to January. The affected areas primarily were those settlements near the floodplain and near river banks. In 2011 and 2012, Valencia City was flooded due to typhoon Washi (locally known as Sendong) and Bopha (locally known as Pablo) which traversed the Bukidnon Province, respectively (NDRRMC, 2011; NDRRMC, 2012).

Process flow chart

Hydrologic and hydraulic models were parameterized using satellite image of land cover and elevation models. The hydrologic model determines the amount of discharge or the rainfall-runoff relationship within the river basin while 2D hydraulic model simulates the behaviour of water flows and precipitation into the river system and floodplain areas. The actual hydrologic data like rainfall and discharge were utilized to calibrate the hydrologic model. The accuracy of the hydrologic model was also examined. 2D hydraulic simulation was conducted using the calibrated hydrologic model which will create the flood depth grid. Depth grid

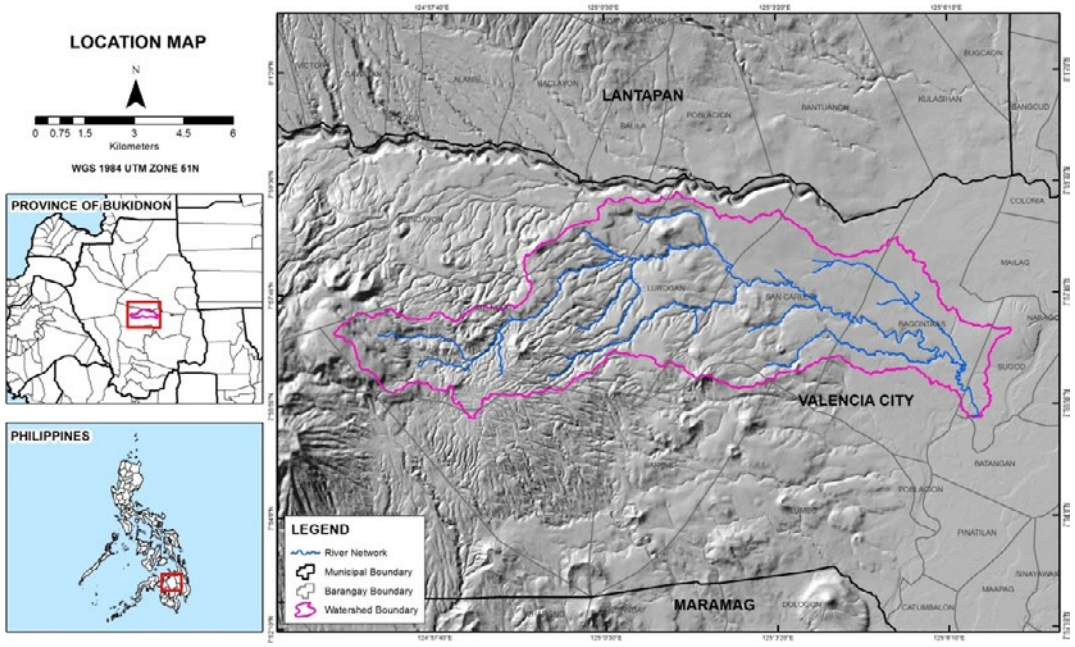

Fg. 1: Geographical location of the study area in Malingon river basin

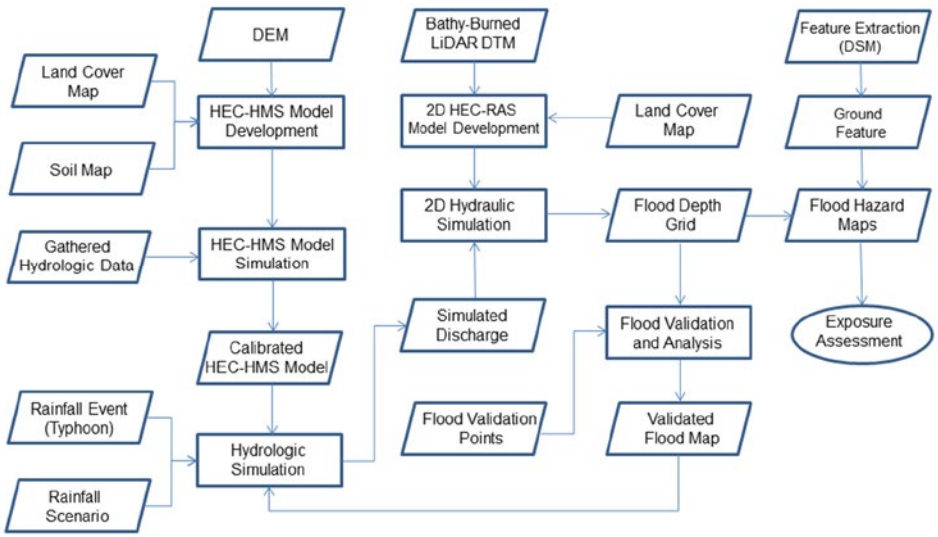

Fig. 2: Process flow of flood hazard mapping

was validated using validation points for accuracy test of the 2D hydraulic model in predicting floods. Flood simulations in different return periods such as 2, 5, 10, 25, 50 and 100-year were applied. The flood depth grids were classified ranging from < 0.5 m, 0.50 m to 1.50 m, and > 1.50 m for low, medium, and high hazards, respectively. Overlay analysis were done using the extracted features from the digital surface model (DSM) to determine the number of exposed features. The process flowchart is shown in Fig. 2 with the trapezoidal shape as the input, the rectangular as the process and oval shape as the output.

Classification of land cover

The Sentinel-2 Level 1C satellite images downloaded from the United States Geological Survey (USGS) Earth Explorer was utilized to generate the Malingon river basin land cover map. The satellite image was acquired last July 16, 2016. The image was pre-processed using "Sen2Cor" plugin in Sentinel Application Platform (SNAP) version 6.0, a tool which process the atmospheric-, terrain and cirrus correction of top-of atmosphere (TOA) Level 1C input data and converts TOA to bottom of atmosphere (BOA) Level 2A products ready for image classification. SNAP is an ideal application for Sentinel-based data processing and analysis with improved extensibility, portability, modular rich client platform, generic data abstraction, tiled memory management, and a graph processing framework (Mueller-Wilm, 2017).The land cover classes were classified using object-based classification and aided with Normalized Difference Vegetation Index (NDVI), an index for visualizing healthy vegetation. The utilization of object-based classification which made easier when exporting into GIS environment and updating the land cover/land use information. This approach combines spectral and spatial information as well as the shape, texture, area, compactness and other context information in the image as the basis for feature classification and produces an output that is composed of grouping pixels or segmentations rather than discrete pixels (Lu *et al.,* 2018; Phiri and Morgenroth, 2017). The generated land cover classes underwent visual inspection to identify obvious misclassification and subjected to manual editing. Accuracy assessment of the classified land cover classes were applied using error matrix. The land cover map was converted to curve number (CN) grid for hydrologic model parameters and Manning's n coefficient map for hydraulic model parameters.

Hydrologic model development and model calibration

The Hydrologic Engineering Center-Hydrologic Modeling System (HEC-HMS) Version 4.0 was used to generate the hydrologic model of Malingon river basin. It is an application which simulates the rainfall-runoff relationship in the watershed with existing condition. The model consists of three components: the basin model that represents the physical watershed, the meteorological model for the weather data, and a set of control specification which represents the computational time settings and simulation period. The basin model was developed using the 10-m Synthetic Aperture Radar-Digital Elevation Model (SAR-DEM) obtained from National Mapping and Resource Information Authority (NAMRIA) and digitized river networks using Google Earth for the delineation of watersheds; and was parameterized using the classified land cover map from Sentinel-2 image and soil data from the Bureau of Soils and Water Management (BSWM). The observed hydro-meteorological data such as discharge and rainfall values are also inputs and necessary for the model simulation. The discharge data was gathered using automatic water level and velocity m together with the river cross-section data at the Malingon Bridge; and the rainfall data from the pre-installed automatic rain gauge at the Barangay Lurugan, Valencia City which is an upstream of the Malingon River. The parameters of the hydrologic model were calibrated by fitting the simulated discharge hydrographs to the actual measured discharge. The actual hydrologic data gathered from December 10, 2017, 00:00 to December 14, 2017, 18:40 were utilized for the model calibration. The model calibration was evaluated using three measures of accuracy namely the Nash-Sutcliffe Coefficient of Model Efficiency (NSE), Percentage Bias (PBIAS), and the root mean square error– observations standard deviation ratio (RSR). The NSE is a normalized measure (–integer to 1.0) that compares the mean error generated by a particular model simulation to the variance of the target output sequence. An NSE value of 1.0 indicates perfect model performance where the model completely simulates the target output, while a value of 0 indicates that the model is, on average, performing only as good as the use of the mean target value as prediction (Nash and Sutcliffe, 1970). The PBIAS measures the average tendency of the simulated values to be larger or smaller than their observed ones. The optimal value of PBIAS is 0.0, with low magnitude values indicating accurate model simulation. Positive values indicate overestimation bias, whereas negative values indicate model underestimation bias (Gupta *et al.,* 1999). The RSR standardizes the root mean square error using the observations' standard deviation and is calculated as the ratio of the root mean square error and the standard deviation of measured data. RSR incorporates the benefits of error index statistics and includes a scaling/normalization factor so that

the resulting statistic and reported values can apply to various constituents. RSR varies from the optimal value of 0 to a large positive value and the lower the RSR, the lower the root mean square error and the better the model simulation performance (Moriasi *et al.,* 2007). These statistical measures were utilized to assess the accuracy of hydrologic simulation by comparing simulated and observed hydrographs which correspond to the existing guidelines and model performance evaluation (Moriasi *et al.,* 2015), shown in Table 1. The hypothetical rainfall event simulations were applied using the Rainfall Intensity Duration Frequency (RIDF) data from the Philippine Atmospheric, Geophysical and Astronomical Services Administration (PAGASA), shown in Table 2. RIDF is a set of information on the likelihood of an event to occur or referred as return periods with different rainfall amount and the duration. The RIDF of the Malaybalay PAGASA Weather Station was used for the hydrologic simulation of hypothetical scenarios in the model.

Two-dimensional hydraulic model development

The Hydrologic Engineering Center River Analysis System (HEC-RAS version 5.0) was used to create the hydraulic model of Malingon River basin. It was designed to perform one-dimensional (1D), two-dimensional (2D), or combined 1D and 2D hydraulic calculations for constructed channels and complex river systems (USACE, 2016; Santillan *et al.,* 2016). The two-dimensionalhydraulic model was developed by producing a 2D flow area or domain representing the floodplain of the river, is shown in Fig. 3. The 2D flow area mesh of Malingon River basin has a total of 99,039 cells with 20-m by 20-m cell size and has an estimated area of 39.84 km^2. The model consisted of four boundary conditions in which two are inflows representing the discharge from upstream rivers (J530 and J467 obtained from the HEC-HMS model), one as the normal depth condition near the outlet (a slope value for discharge distribution), and one boundary condition for the precipitation that falls to the 2D area as inputs into the HEC-RAS 2D hydraulic model to predict or estimate flood depths and extents. With the use of break lines or the abrupt changes in elevation which represents the roads and river banks, the 2D flow area was computed to create the computational mesh or cells. The 1-m resolution terrain model was utilized as the main source of elevation data. Parameterization of the HEC-RAS model utilized the land cover information by extracting the Manning's roughness coefficients, and these values were used to calculate the hydraulic table properties of flood simulation area.

Flood depth generation and hazard classification

There were two inflow boundary condition locations which represent the flow hydrograph that enters the hydraulic model. The unsteady flow analysis module of HEC-RAS was applied and the simulated flow hydrographs coupled with the precipitation data were used to generate flood depth and extent. Maximum flood depth grids were created in every simulation of each return period.

Table 1: Model performance evaluation (Moriasi *et al.,* 2015)

Remarks	Statistical criterion		
	NSE	PBIAS	RSR
Very Good	0.75 <NSE< 1.00	PBIAS< ± 10	0.00 <RSR< 0.50
Good	0.65 <NSE< 0.75	± 10 <PBIAS< ± 15	0.50 <RSR< 0.60
Satisfactory	0.50 <NSE< 0.65	± 15 <PBIAS< ± 25	0.60 <RSR< 0.70
Unsatisfactory	NSE< 0.50	PBIAS> ± 25	RSR> 0.70

Table 2: Values of the different hypothetical rainfall events based on local RIDF data

Return periods	Duration							
(Year)	5 min	15 min	1 h	2 h	3 h	6 h	12 h	24 h
2	9	21.4	47.8	63.7	73.5	90.2	103.4	112.8
5	13.4	34	78.4	100.8	114.3	130.2	143.2	153.6
10	16.3	42.4	98.6	125.3	141.4	156.7	169.6	180.7
25	20	52.9	124.1	156.3	175.5	190.1	202.8	214.8
50	22.7	60.8	143	179.3	200.9	214.9	227.5	240.2
100	25.4	68.6	161.8	202.2	226	239.5	252	265.3

The resulting flood depth grids were exported into the GIS software and categorized into flood hazards which corresponds to varying levels (Low hazard: less than 0.50 m, Medium hazard: 0.50 m to 1.50 m, and High hazard; greater than 1.50 m).

Flood validation survey and error analysis

Flood validation survey was conducted to obtain flooding information from the local people through personal interview within the river basin whether they were flooded or not flooded in a certain typhoon event. For this study, Tropical Storm Sendong (international name Tropical Storm Washi) flooding information was gathered. It was also conducted to assess the accuracy of the Malingon HMS-RAS model in generating flood hazard maps by rebuilding historical events. Interpolated historical rainfall data of Tropical Storm Sendong in 2011 gathered from Butuan, Lumbia, Malaybalay, Cotabato, Davao and General Santos PAGASA station was utilized, since there were no available rainfall data within the basin that time. The generated flood map from Tropical Storm Sendong was compared to the validation points gathered within the Malingon River basin. The accuracy computation used the confusion matrix approach which compares model result against actual collected data (Dzikovska *et al.,* 2012; Doreswamy and Hemanth, 2012; Bowes *et al.,* 2012). Another accuracy measure used is the F-measure known as harmonic mean which determines the fitness of the simulated flood extent to the actual setting on the ground (Santillan*et al.,* 2016; Lu *et al.,* 2018; Guo *et al.,* 2018). If F=1, means that the reference and compared flooding extents coincide exactly, while F=0 means that no overlap exists between the reference and compared flooding extents. Flooding extents generated by the 2D hydraulic model can be assessed either as "Good Fit" with F-value of greater than or equal to 0.7, "Intermediate Fit" with F-value of less than 0.7 but less than or equal to0.5, or "Bad Fit" with F value of less than 0.5 (Breilh *et al.,* 2013). To determine the error difference of the simulated flood depth and the actual gathered flood height in the field, the root mean square error (RMSE) was also applied in the study with acceptable range of less than 0.50 m.

Feature extraction

The ground features in Malingon River basin were extracted from the 1m high resolution LIDAR-

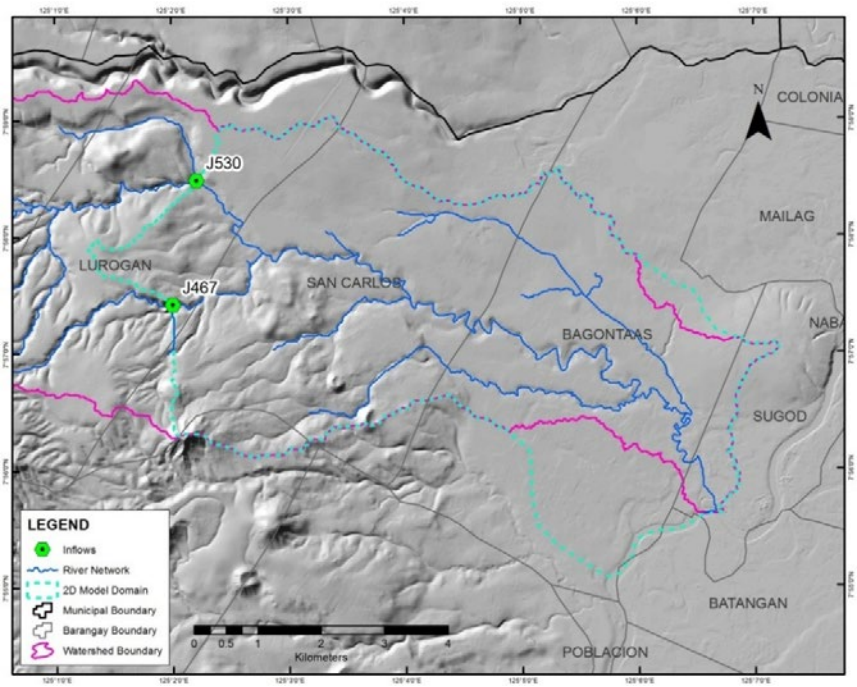

Fig. 3: 2d model domain (floodplain) of Malingon River for HEC-RAS

derived digital surface model (DSM) gathered by the University of the Philippines-Diliman (UPD) last 2016. These features refer to ground structures which consist of buildings or houses only. Within the 2D model domain of Malingon River floodplain is shown in Fig. 4, a total of 7,184 extracted building features. The extraction was aided with high-resolution satellite images from Google Earth and Google Street View, and validated using geo-tagged photos. Extracted buildings were utilized as a primary input for flood exposure assessment.

Scenario flood simulation and flood exposure assessment

Output hydrographs from calibrated HMS model of Malingon River using different rainfall scenarios were utilized as an input for the validated 2D RAS model together with land cover map for roughness coefficient. The generated flood depth grids were classified according to different flood hazards which repeat the process. The extracted features from the DSM and the flood hazard maps of different rainfall scenarios were utilized to flood exposure assessment. Overlay analysis were applied to determine the number of buildings exposed to flood hazards.

RESULTS AND DISCUSSION

Land cover map

The land cover map of Malingon river was generated utilizing the available Sentinel-2 satellite image and classified into 6 categories such as agricultural land, bare land, built-up area, forest, grassland and water is shown in Fig. 5.It has an overall accuracy of 96.7% and Kappa coefficient of 96.3%. The agricultural land is the dominant land cover within Malingon river basin with 60.92 % and followed by bare land or fallow area with 11.76%. This means that the watershed is agriculturally active of which the economy is more on agricultural production. As it is shown in Table 3, the area in square kilometres (km^2) and percentage of each land cover description.

Calibration of hydrologic model and simulation of rainfall scenarios

Discharge data collected in Malingon Bridge and the rainfall data in Barangay Lurugan were utilized

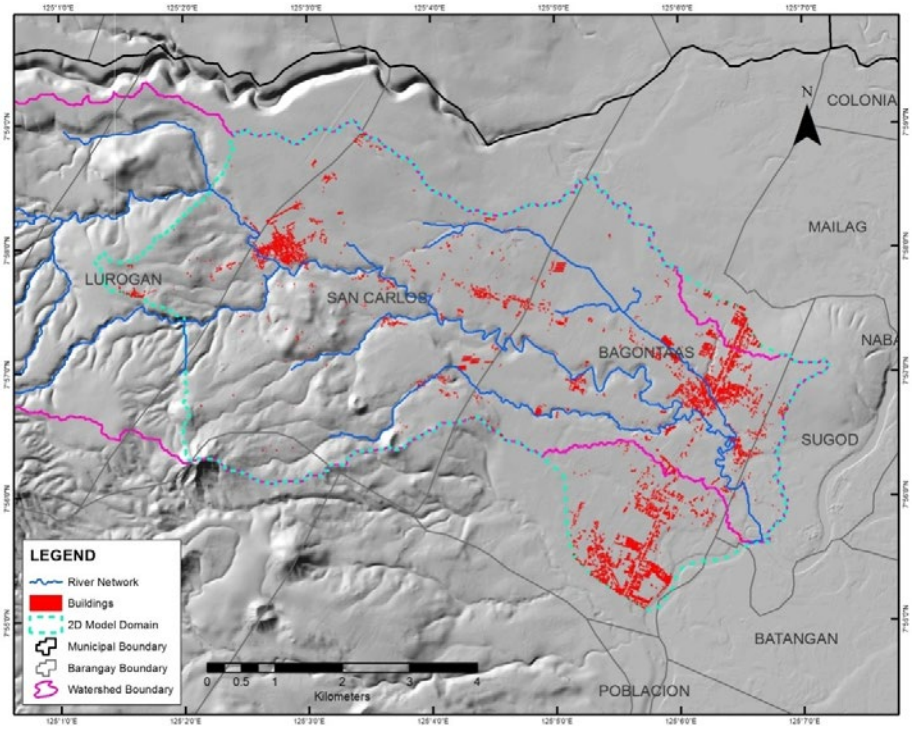

Fig. 4: Extracted building features within the 2d model domain of Malingon river basin

Table 3: Area and percent per land cover in Malingon River basin

Land cover name	Area (km^2)	Percentage
Agricultural Land	43.66	60.92
Bare Land	8.43	11.76
Built-up Area	1.86	2.60
Forest	13.29	18.55
Grassland	4.40	6.14
Water	0.02	0.03
Total	71.68	100.00

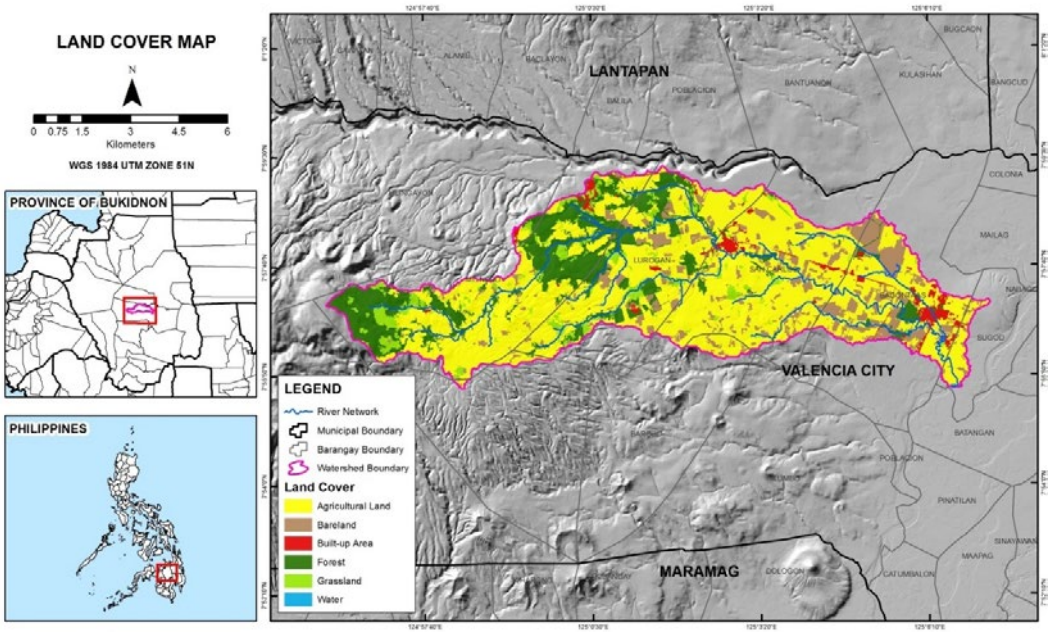

Fig. 5: Malingon River basin land cover map 2016

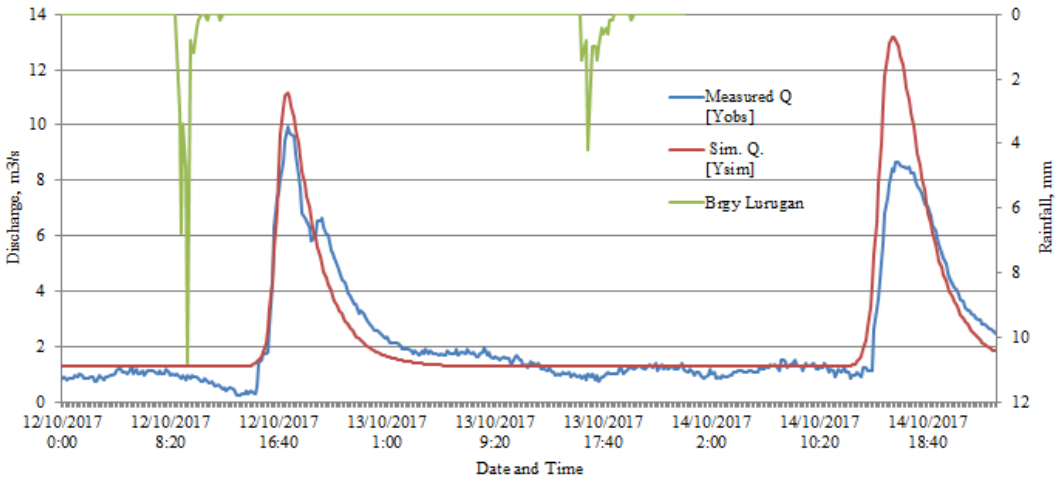

Fig. 6: Calibration result of Malingon river basin HEC-HMS model using the observed discharge

to calibrate the model. The calibration results of Malingon HEC-HMS model is shown in Fig. 6. The overall performance of the model based on the Moriasi *et al.* (2015)'s evaluation guidelines and model performance, with resulting values of NSE = 0.78, PBIAS = -8.62, and RSR = 0.46 are considered "very good". This implies that the HEC HMS model of Malingon River is ready for utilization in simulating flow hydrographs using extreme rainfall events. Fig. 7 shows the resulting 24-h simulated hydrographs within the inflows of J530 and J467 using the calibrated HEC HMS model and the different rainfall scenarios. The

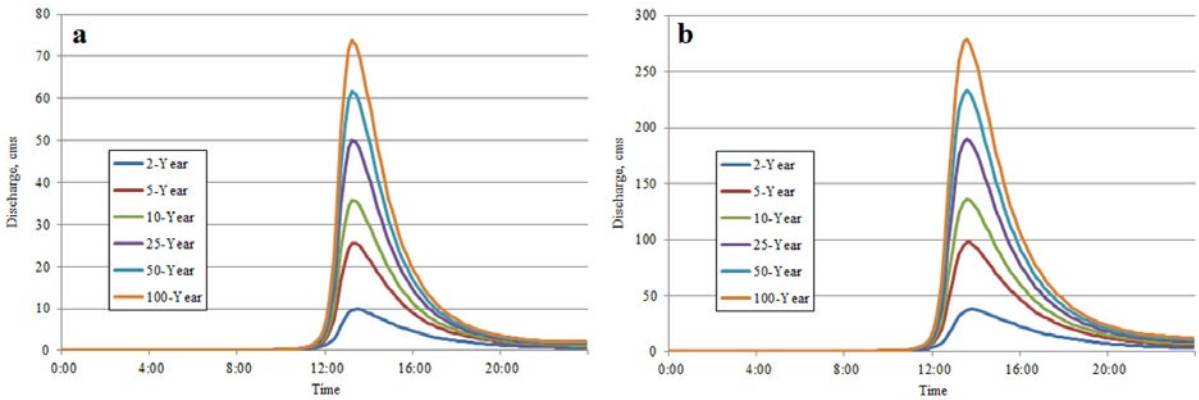

Fig. 7: Simulated hydrographs using the calibrated HEC HMS model of Malingon river and rainfall scenarios (a: J467 and b: J530)

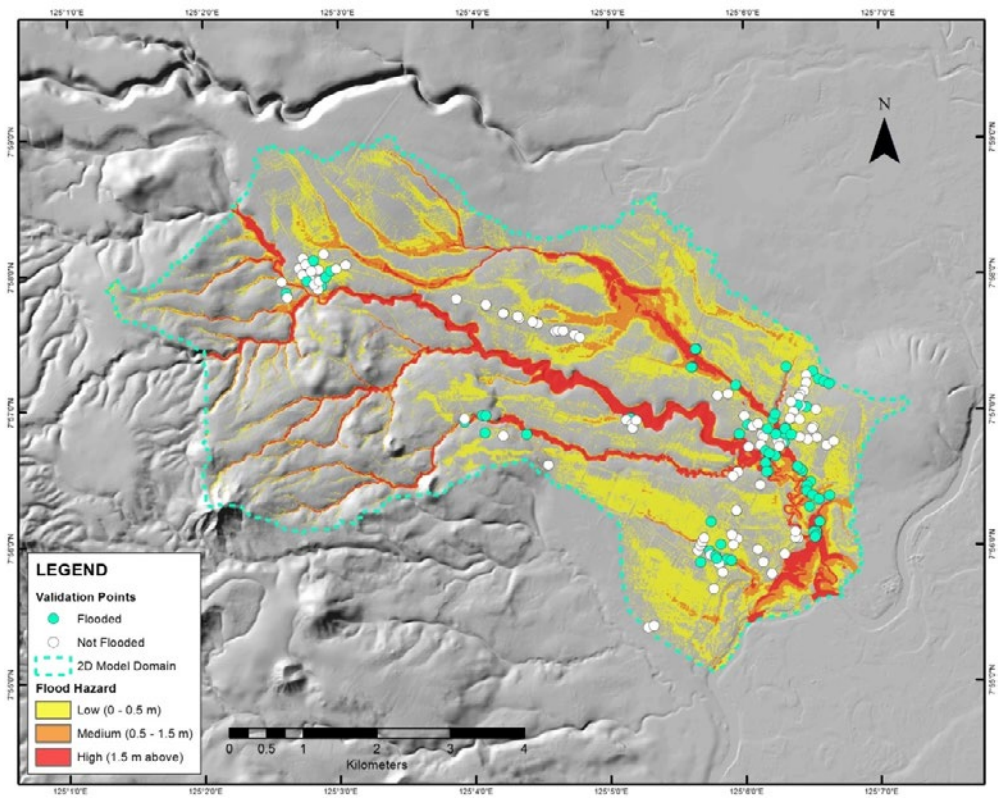

Fig. 8: Flood validation points of Malingon river in tropical storm Sendong flood hazard map

peak flow of the J530 is larger than the peak flow of J467, since the catchment area of J530 is larger than J467. This simulated hydrographs were utilized for flood simulation in HEC RAS model of Malingon river basin. The amount of rainfall return period is directly proportional to the amount of discharge within the two inflows with increasing trend.

Flood validation and error analysis

Reconstruction of flooding extent during Tropical Storm Sendong was applied and utilizing the flooding information and validation points of the same event within the floodplain of Malingon River to determine the accuracy of the Malingon 2D HEC RAS model in generating flood hazard maps

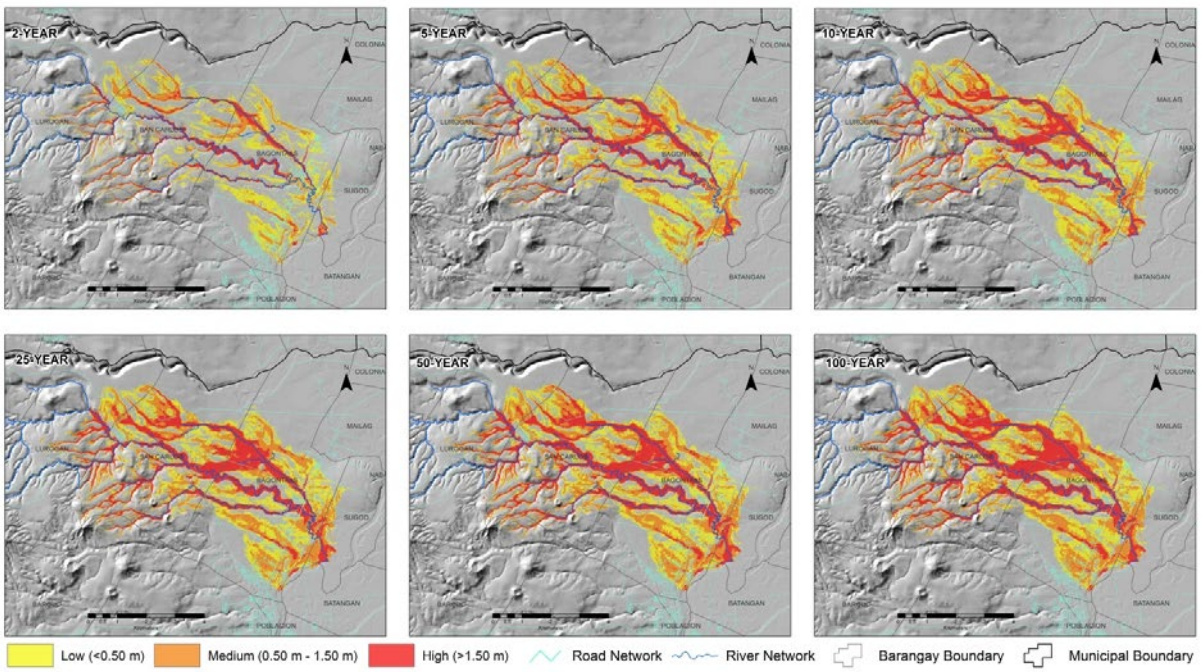

Fig. 9: Flood hazard maps of Malingon River in different return periods

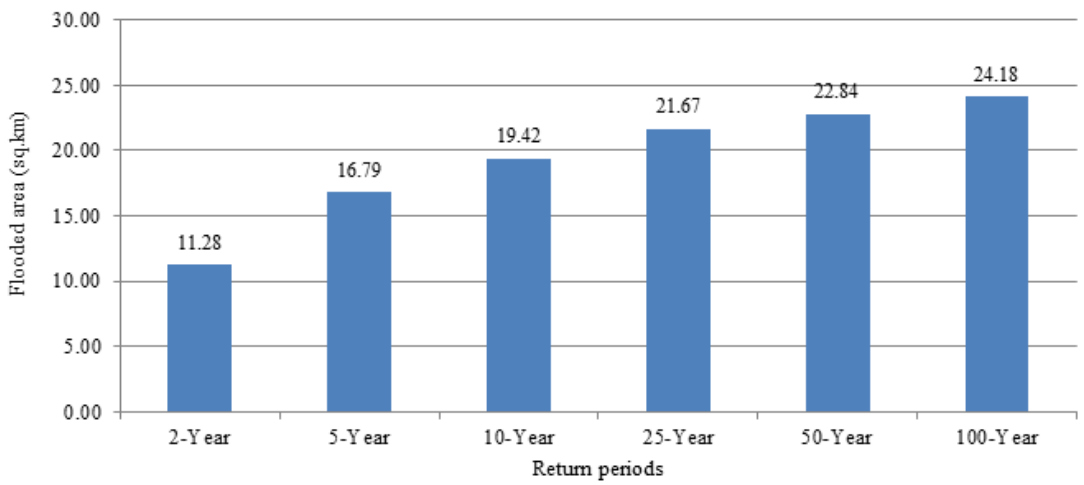

Fig. 10: Area flooded of Malingon River in different return periods

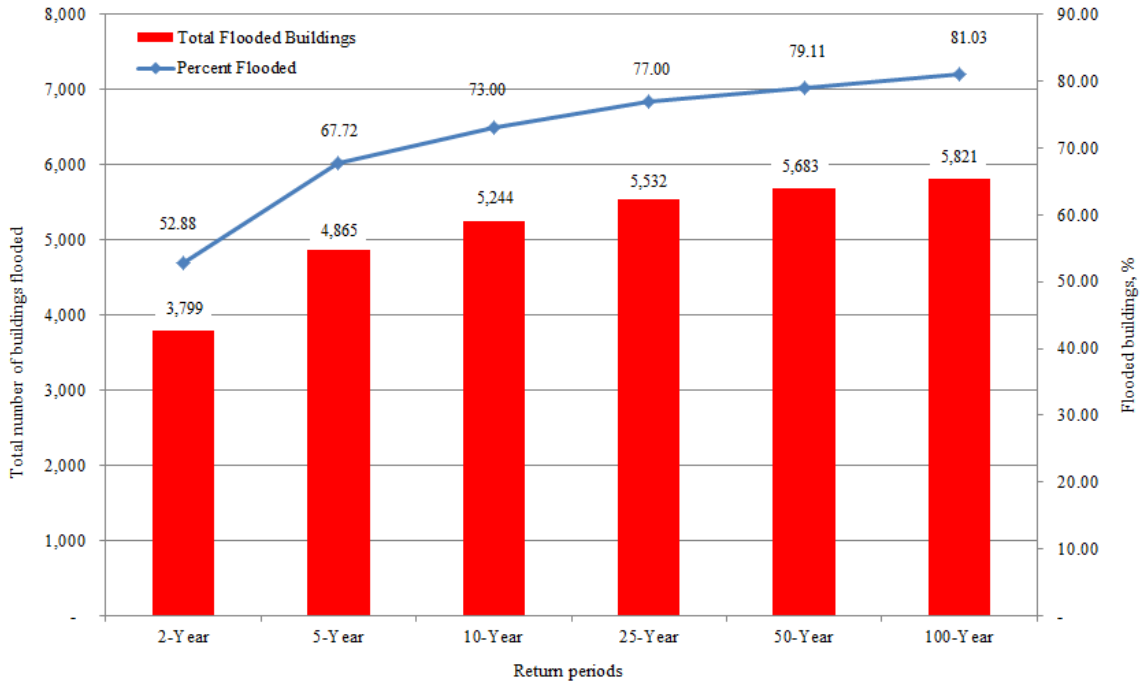

Fig. 11: Total number of flooded buildings and percentage in different return periods

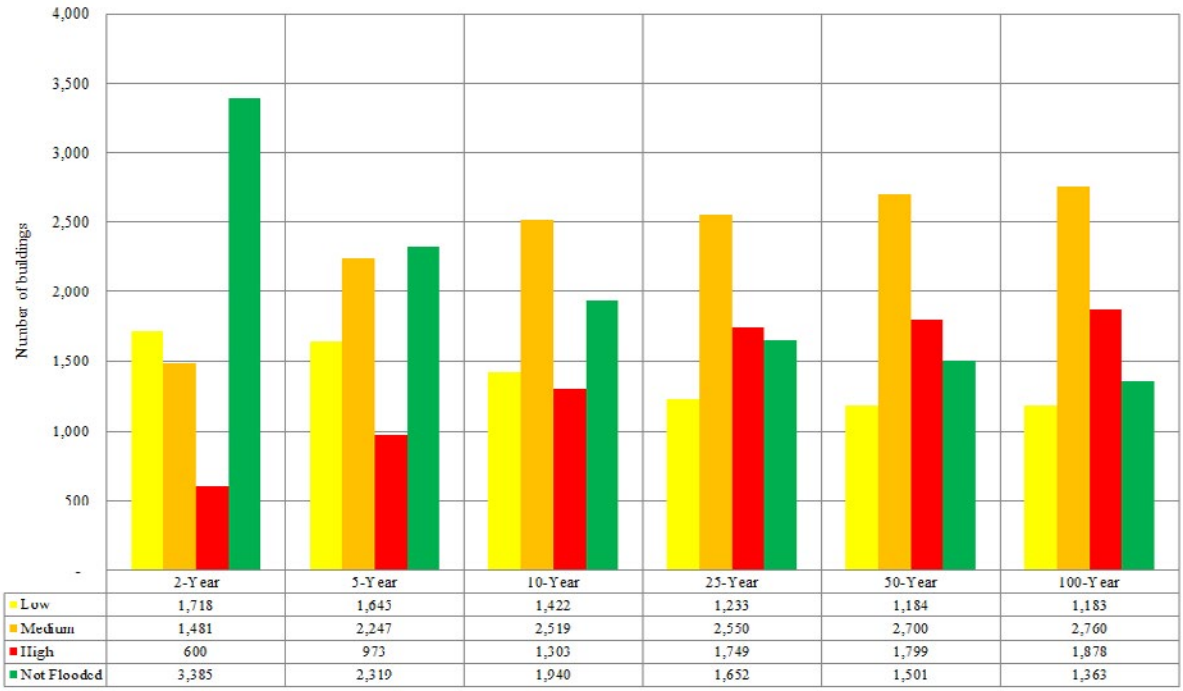

	2-Year	5-Year	10-Year	25-Year	50-Year	100-Year
Low	1,718	1,645	1,422	1,233	1,184	1,183
Medium	1,481	2,247	2,519	2,550	2,700	2,760
High	600	973	1,303	1,749	1,799	1,878
Not Flooded	3,385	2,319	1,940	1,652	1,501	1,363

Fig. 12: Number of flooded buildings per hazard level per return period

(Fig. 8). Based on the confusion matrix analysis, the accuracy of the Malingon 2D HEC-RAS model in simulating flood extent and depth is 80.5%, which implies that the model can generate any flood event from any rainfall event can be 80.5% accurate. The result in F measure analysis was 0.56, which means that the flood map generated by the models is within the "Intermediate fit". The calculated root mean square error is 0.47 m and within the acceptable range of less than 0.50 m, indicates that the model over predict the flood depth estimation by 0.47 m.

Generated flood hazard maps

After the Malingon 2D HEC RAS model passed the flood error analysis, the model utilized the simulated hydrographs and extreme rainfall values from the Malingon HEC HMS model to generate flood hazard maps in different return periods is shown in Fig. 9. There is an increasing trend of the flood extents as return period increases.The 2D model domain of Malingon River has a total area of 39.84 km^2. The 2-y return period has the smallest flooded area with 28.3% and accounts to 11.28 km^2. In addition, the 100-y return period, 60.67% of the 2D model domain total area was flooded which accounts to 24.17 km^2 and the largest area flooded (Fig. 10). This means that the return periods (amount of rainfall) are directly proportional to the flood extents. All of the generated flood hazard maps are assumed to be an 80.5% accurate based on the error analysis of the flood map validation using tropical storm Sendong flood information.

Exposure Assessment

Results show that the number of flooded buildings increases with the increase of rainfall amount as modelled using different return periods (Fig. 11). The total number of buildings sampled in Malingon River floodplain is 7,184. The 100-y return period has the most number of flooded buildings with 81.03% which account to 5,821 buildings. This implies that in extreme scenarios with 1% chance probability every year, more than 80% of the buildings will be flooded. For smallest number of flooded buildings was in 2-y return period accounting to 3,799 buildings with 52.88% from the total number of building sampled. This means that more than half of the sampled buildings will be flooded in 50% chance probability every year. Most of them located near the downstream portion and near the river banks. The results of assessing the exposed buildings to flooding per hazard level per return periods in Malingon river floodplain is shown in Fig. 12.

The graph shows an inverse proportion of not flooded buildings and the number of flooded buildings in low hazard areas. On the other hand, in the medium and high hazard level in orange and red colors, respectively, there is an increasing trend was observed in the number of flooded buildings. For 2-y and 100-y return period scenarios, an increase of 46% and 68% flooded buildings for medium and high hazard level, respectively, were observed. Expectedly, assessment showed that exposed features have been increased with the extent of flooding in the area. All of the flooded and not flooded buildings per hazard level in different return periods having an accuracy of 80.5% based on the results of error analysis of the flood validation using Tropical Storm Sendong flood information.

CONCLUSION

The study has generated important geospatial datasets and information to include land cover, soil, elevation models, rainfall, and discharge, among others, as primary inputs in flood modeling. The overall model performance was fitted showing acceptable accuracy both for the hydrologic model calibration and hydraulic models validation. Hydrologic model performance was tested using NSE, PBIAS, and RSR statistics with values of 0.78, -8.62, and 0.46, respectively. The respective increasing trends in the amount of discharge, flood extents and number of buildings exposed to flood with the increasing amount of extreme rainfall events (return periods) were described in this study. Highly detailed flood hazard maps at different return period scenarios were generated which will be made available to target beneficiaries like LGUs and other agencies. The generated hazard maps and flood simulations help local community to understand the dissimilarities of the impacts of different rainfall amount occurring in the floodplains. Output of the study served as valuable input in the formulation of science-based policy recommendations that shall be integrated into the local and regional policies on Disaster Risk

Reduction Management (DRRM) Plans and actions. This initiative is believed to contribute in building disaster-resilient communities towards sustainable development not only in the floodplain of Malingon but for the entire Island of Mindanao.

ACKNOWLEDGMENTS

This study is an output of the Central Mindanao University (CMU) GeoSAFER: Northern Mindanao/ Cotabato Project 2 under GeoSAFER Mindanao Program supported by the funding agency Department of Science and Technology-Philippine Council for Industry, Energy and Emerging Technology Research and Development (DOST-PCIEERD) and to the local government units of the Province of Bukidnon for the counterpart. Authors also thank the CMU administration for the continued support as well as the University of the Philippines Disaster Risk and Exposure for Mitigation (UP DREAM) and Phil-LIDAR Programs for the SAR-DEM, the LIDAR DTM, and DSM datasets.

CONFLICT OF INTEREST

The authors declare that there are no conflicts of interest regarding the publication of this manuscript. In addition, the ethical issues; including plagiarism, informed consent, misconduct, data fabrication and/or falsification, double publication and/or submission, redundancy has been completely observed by the authors.

ABBREVIATIONS

%	Percent
1D	one-dimensional
2D	two dimensional
BOA	bottom of atmosphere
BSWM	Bureau of Soils and Water Management
CN	Curve number
CMU	Central Mindanao University
DSM	Digital surface model
DOST-PCIEERD	Department of Science and Technology- Philippine Council for Industry, Energy and Emerging Technology Research and Development
Geo-SAFER	Geo-Informatics for the systematic assessment of flood effects and risks
GIS	Geographic information system
h	hour
HEC-HMS	Hydrologic Engineering Center-Hydrologic Modeling System
HEC-RAS	Hydrologic Engineering Center-River Analysis System
J467	First inflow element
J530	Second inflow element
km^2	Kilometre square
LIDAR	Light detection and ranging
m	meter
min	minute
NDVI	Normalized difference vegetation index
NSE	Nash-Sutcliffe coefficient of model efficiency
PAGASA	Philippine Atmospheric, Geophysical and Astronomical Services Administration
PAR	Philippine Area of Responsibility
PBIAS	Percentage bias
RIDF	Rainfall intensity duration frequency
RMSE	root mean square error
RSR	observations standard deviation ratio
SAR-DEM	Synthetic aperture radar digital elevation model
SNAP	Sentinel Application Platform
TOA	top-of atmosphere
UPD	University of the Philippines-Diliman
UP DREAM	University of the Philippines Disaster Risk and Exposure for Mitigation

REFERENCES

Abolghasem, M.; Golamali, F.; Mohsen; Maliheh, S., (2014). Modern applied science; impact of land use change on river floodplain using public domain hydrologic model. Canadian Centre of Science and Education, 8(5): 80-86 (**7 pages**).

Acosta, J.E.; De Leon, R.K.; Hollite, J.R., (2017). Flood modeling using GIS and lidar of Padada River in south eastern Philippines. In Proceedings of the 3rd International Conference on Geographical Information Systems Theory, Appl. Manage., GISTAM 2017: 301-306 (**6 pages**).

Acosta, L.A.; Eugenio, E.A.; Macandog, P.B.M.; Magcale-Macandog, D.B.; Lin, E.K.H., (2016). Loss and damage from typhoon-induced floods and landslides in the Philippines: community perceptions on climate impacts and adaptation options. Int. J. Global Warming, 9(1): 33-65 (**33 pages**).

ADRC, (2009). Philippines' country profile. Asian Disaster Reduction Centre, 1-38 (**38 pages**).

Akbari, G.H.; Nezhad, A.H.; and Barati, R., (2012). Developing a model for analysis of uncertainties in prediction of floods. J. Adv. Res., 3(1): 73-79 (**7 pages**).

Ban, H.J.; Kwon, Y.J.; Shin, H.; Ryu, H.S.; Hong, S., (2017). Flood monitoring using satellite-based RGB composite imagery and refractive index retrieval in visible and near-infrared bands. Remote Sens. 9: 313-331 (**19 pages**).

Bowes, D.; Hall, T.; Gray, D., (2012). Comparing the performance of fault prediction models which report multiple performance measures: Recomputing the confusion matrix. University of Hertfordshire Research Archive, 1-10 (**10 pages**).

Breilh, J. F.; Chaumillon, E.; Bertin, X.; Gravelle, M., (2013). Assessment of static flood modeling techniques: application to contrasting marshes flooded during Xynthia (western france). Natural Hazards and Earth System Sci., 13(6), 1595-1612 (**18 pages**).

Costabile, P.; Macchione, F., (2015). Enhancing river model set-up for 2-d dynamic flood modelling. Environ. Model. Software, 67: 89-107 (**19 pages**).

Costas, A.; Erin, X.D.; Sowmaya, N.; Ravi, A. P.; Ying, Z., (2017). Flood risk assessment in urban areas based on spatial analytics and social factors. Geosciences, 7: 123-137 (**15 pages**).

Das, T.; Maurer E.P.; Pierce D.W.; Dettinger M. D.; Cayan D.R., (2013). Increases in flood magnitudes in California under warming climates. J. Hydrol., 501: 101-110 (**10 pages**).

Doreswamy, D.; Hemanth, K.S., (2012). Performance evaluation of predictive classifiers for knowledge discovery from engineering materials data sets. Artificial intelligent systems and machine learning. CIIT Journal, 1-8 (**8 pages**).

Doroteo, H.J., (2015). Philippines: disaster risk profile and disaster risk reduction (DRR) framework: natural calamities. University of Oviedo, Asturias, Spain, 1-46 (**46 pages**).

Dzikovska, M.O.; Bell, P.; Isard, A.; Moore, J.D., (2012). Evaluating language understandingaccuracy with respect to objective outcomes in a dialogue system. Proceedings of the 13th Conference of the European Chapter of the Association for Computational Linguistics. 471–481 (**11 pages**).

FAO, (2011). Philippines: natural disasters of all kinds rank high in the Philippines. FAO, 1-12 (**12 pages**).

Guo, H.; Zhou, J.; Wu, C., (2018). Imbalanced learning based on data-partition and SMOTE. Information. 9: 238-259 (**22 pages**).

Gupta, H. V.; Sorooshian, S.; Yapo. P. O., (1999). Status of automatic calibration for hydrologic models: Comparison with multilevel expert calibration. J. Hydrologic Eng. 4(2): 135-143 (**9 pages**).

Haq, M.; Akhtar, M.; Muhammad, S.; Paras, S.; Rahmatullah, J., (2012). Techniques of remote sensing and GIS for flood monitoring and damage assessment: a case study of Sindh Province, Pakistan. The Egypt. J. Remote Sens. Space Sci., 15(2): 135-141 (**7 pages**).

IFRC, (2017). Emergency appeal operation update Philippines: tropical storm Tembin. International Federation of Red Cross and Red Crescent Societies, 1-23 (**23 pages**).

JICA, (2015). Country report Philippines: natural disaster risk assessment and area business continuity plan formulation for industrial agglomerated areas in the ASEAN Region. Japan International Cooperation Agency, 1-123 (**131 pages**).

Jung, Y.; Dongkyun, K.; Dongwook, K.; Munmo, K.; Lee, S.O., (2014). Simplified flood inundation mapping based on flood elevation-discharge rating curves using satellite images in gauged watersheds. Water. 6: 1280-1299 (**20 pages**).

Kherde, R.V.K.; Sawant, P.H., (2013). Integrating geographical information systems (GIS) with hydrological modelling – applicability and limitations. Int. J. Eng. Technol., 5(4): 3374-3381 (**8 pages**).

Koutroulis A.G.; Tsanis I.K., (2010). A method for estimating flash flood peak discharge in a poorly gauged basin: case study for the 1314 January 1994 flood, Giofiros basin, Crete, Greece. J. Hydrol., 385: 150-164 (**15 pages**).

Lu, L.; Tao, Y.; Di, L., (2018). Object-based plastic-mulched landcover extraction using integrated sentinel-1 and sentinel-2 data. Remote Sens., 10(11): 1-18 (**18 pages**).

Lu, T.; Ming, D.; Lin, X.; Hong, Z.; Bai, Z.; Fang, J., (2018). Detecting building edges from highspatial resolution remote sensing imagery using richer convolution features network. Remote Sens., 10: 1496-1514 (**19 pages**).

LWR, (2017). The Philippines: typhoon Tembin January 8, 2018: No. 3 situation report. Lutheran World Relief. Technical Report, 1-2 (**2 pages**).

Makinano-Santillan, M.; Santillan, J.R.; Amora, A.M.; Marqueso, J.T.; Cutamota, L.C.; Serviano, J.L.; Oconer, P.C.R.; Makinano, R.M., (2015). Assessing the impacts of flooding in Tago River basin, mindanao, philippines through integration of high-resolution elevation datasets, land sat image analysis, and numerical modeling. In: 36th Asian Conference on Remote Sensing 2015 (ACRS 2015): Fostering Resilient Growth in Asia, Quezon City, Metro Manila, Philippines, 3: 1606-1617 (**12 pages**).

McDougall K.; Temple-Watts, P., (2012). The use of Lidar and volunteered geographic information to map flood extents and inundation. ISPRS Annals of the Photogrammetry, Remote Sensing and Spatial Information Sciences, Volume I-4, 2012 XXII ISPRS Congress, Melbourne, Australia, 251-256 (**6 pages**).

Moriasi, D.N.; Arnold, J.G.; Van Liew, M.W.; Bingner, R.L.; Harmel, R.D.; Veith, T.L., (2007). Model evaluation guidelines for systematic quantification of accuracy in watershed simulations.

Trans. ASABE, 50, 885–900 (**16 pages**).

Moriasi, D.N.; Gitau, M.W.; Pai, N.; Daggupati, N., (2015). Hydrologic and water quality models: performance measures and evaluation criteria. Am. Soc. Agric. Biol. Eng., 58(6): 1763-1785 (23 pages).

Mueller-Wilm, U., (2017). Sen2cor configuration and user manual v2.4. European Space Agency, 1-53 (**53 pages**).

Nash, J.E.; Sutcliffe, J.V., (1970). River flow forecasting through conceptual models part I—A discussion of principles. J. Hydrol., 10, 282–290 (**9 pages**).

NDRRMC, (2011). Ndrrmc update sitrep no.4 re: effects of tropical storm "Sendong" (Washi). National Disaster Risk Reduction and Management Council. Technical Report, 1-17 (**17 pages**).

NDRRMC, (2012). Ndrrmc update sitrep No.38 re effects of typhoon "Pablo" (Bopha). National Disaster Risk Reduction and Management Council. Technical Report, 1-54 (**54 pages**).

NDRRMC, (2013). Ndrrmc update sitrep No.12 effects of typhoon "Volanda" (Haiyan). National Disaster Risk Reduction and Management Council. Technical Report, 1-42 (**42 pages**).

NDRRMC, (2014). Ndrrmc sitrep No.20 re effects of typhoon "Ruby" (Hagupit). National Disaster Risk Reduction And Management Council. Technical Report, 1-38 (**38 pages**).

NDRRMC, (2015). Ndrrmc update sitrep No.26 re preparedness measures and effects of typhoon "Lando" (Koppu). National Disaster Risk Reduction and Management Council. Technical Report, 1-132 (**132 pages**).

NDRRMC, 2017. Ndrrmc update sitrep No.26 re preparedness measures and effects of typhoon "Vinta" (Tembin). National Disaster Risk Reduction and Management Council. Technical Report, 1-41 (**41 pages**).

OCHA, (2015). Philippines: typhoon Koppu situation report No. 4. Office for the Coordination of Humanitarian Affairs, 1-3 (**3 pages**).

Phiri, D.; Morgenroth, J., (2017). Developments in landsat land cover classification methods: a review. Remote Sens., 9(9): 1-25 (**25 pages**).

Rola, A.C.; Suminguit, V.J.; Sumbalan, A.T., (2004). Realities of the watershed management approach: the Manupali watershed experience. Philippine Institute for Development Studies (PIDS), Philippines. PIDS Discussion Paper Series, No. 2004-23, 1-39 (**39 pages**).

Saleh, A.S.; Al-Hatrushi, S.M., (2009). Torrential flood hazards and management, in Wadi Aday Muscat area, Sultanate of Oman, a GIS approach. Egypt J. Remote Sens. Space Sci., 12: 71-86 (**16 pages**).

Santillan, J.R.; Amora, A.M.; Makinano-Santillan, M.; Marqueso, J. T.; Cutamora, L. C.; Serviano, J. L.; and Makinano, R.M., (2016). Assessing the impacts of flooding caused by extreme rainfall events through a combined geospatial and numerical modeling approach, Int. Arch. Photogramm. Remote Sens. Spatial Inf. Sci., XLI-B8, 1271-1278 (**9 pages**).

Turner, A.B.; Colby, J.D.; Csontos, R.M.; Batten M., (2013). Flood modelling using a synthesis ofmulti-platform Lidar data. Water, 5: 1533-1560 **(28 pages)**.

UNOCHA, (2017). Philippines: destructive tropical cyclones from 2006 to 2016. United Nations Office for the Coordination of Humanitarian Affairs, 1 **(1 page).**

USACE, (2008). Hydrologic modelling system Hec-Hms applications guide (2008). United States Army Corps of Engineers, Hydrologic Engineering Centre, Davis, California, USA, 1-118 **(118 pages).**

USACE, (2016). HEC-RAS river analysis system. 2d modelling user's manual version 5.0, United States Army Corps of Engineers Institute for Water Resources Hydrologic Engineering Centre (HEC) Davis, California, USA, 1-171 **(171 pages)**.

Vojtek, M.; Vojteková, J., (2016). Flood hazard and flood risk assessment at the local spatial scale: a case study, Geomatics. Natural Hazards Risk, 7(6): 1973-1992 **(20 pages).**

Yoshimoto, S.; Amarnath, A., (2017). Applications of satellite-based rainfall estimates in flood inundation modelling: a case study in mundeni Aru river basin, Sri Lanka. Remote Sens. 9: 998-1013 **(16 pages).**

AUTHOR (S) BIOSKETCHES

Talisay, B.A.M., B.Sc., Senior Science Research Specialist, GeoSAFER Northern Mindanao/Cotabato Project, College of Forestry and Environmental Science, Central Mindanao University, Musuan, Maramag 8710, Bukidnon, Philippines.
Email: *bryanallan.talisay@gmail.com*

Puno, G.R., Ph.D., Associate Professor, and Project Leader GeoSAFER Northern Mindanao/ Cotabato Project, College of Forestry and Environmental Science, Central Mindanao University, Musuan, Maramag 8710, Bukidnon, Philippines. Email: *punogeorge@gmail.com*

Amper, R.A.L., B.Sc., University Researcher, GeoSAFER Northern Mindanao/ Cotabato Project
College of Forestry and Environmental Science, Central Mindanao University, Musuan, Maramag 8710, Bukidnon, Philippines.
Email: *roseangelica_amper@yahoo.com*

HOW TO CITE THIS ARTICLE

Talisay, B.A.M., Puno, G.R., Amper, R.A.L., (2019). Flood hazard mapping using combined hydrologic-hydraulic models and geospatial technologies in an urban area. Global J. Environ. Sci. Manage., 5(2): 139-154.

DOI: 10.22034/gjesm.2019.02.01

url: https://www.gjesm.net/article_33289.html